Dalton Transactions

Accepted Manuscript

ROYAL SOCIETY OF CHEMISTRY

www.rsc.org/dalton

Graphical Abstract

Three Zn(II)-complex-supporting Strandberg-type molybdophosphates have been synthesized, and they represent the first example of Strandberg-type POMs used as catalysts for organic reaction.

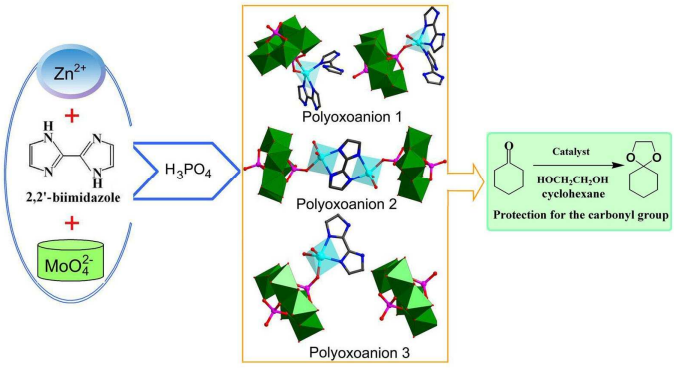

Cite this: DOI: 10.1039/c0xx00000x

www.rsc.org/xxxxxx

ARTICLE TYPE

Three molybdophosphates based on Strandberg-type anions and Zn(II)-H_2biim/H_2O subunits: syntheses, structures and catalytic properties

Zi-Liang Li, Ying Wang, Lan-Cui Zhang*, Jian-Ping Wang, Wan-Sheng You, and Zai-Ming Zhu*

Received (in XXX, XXX) Xth XXXXXXXXX 20XX, Accepted Xth XXXXXXXXX 20XX

DOI: 10.1039/b000000x

Three new inorganic-organic hybrid compounds based on Strandberg-type anions and Zn(II)-H_2biim/H_2O subunits, namely $\{H_4(H_2biim)_3\}[Zn(H_2biim)(H_3biim)(H_2O)(HP_2Mo_5O_{23})]_2{\cdot}3H_2O$ (**1**), $\{H_9(H_2biim)_7\}[(\mu\text{-biim})\{(Zn(H_2O)_2)_{0.5}(HP_2Mo_5O_{23})\}_2]{\cdot}7H_2O$ (**2**) and $\{H_7(H_2biim)_7\}[Zn(H_2biim)(H_2O)_2(HP_2Mo_5O_{23})][H_2P_2Mo_5O_{23}]{\cdot}8H_2O$ (**3**) (H_2biim = 2,2'-biimidazole) have been synthesized in aqueous solutions and characterized. They were also used as efficient and reusable catalysts for the protection of carbonyl compound. Their fascinating structural features are that mono Zn(II)-supporting biphosphopentamolybdate ($\{P_2Mo_5\}$) clusters exist in their crystal structures, and the nitrogen donor ligand H_2biim exhibits three different coordination modes in these three compounds, respectively: for **1**, two 2,2'- biimidazole molecules, as mono- and bidentate ligands coordinate to the same Zn(II) ion; for 2, one bi-negative tetradentate ligand μ-biim bridges two Zn(II) ions; while for **3**, one neutral bidentate H_2biim ligand links one Zn(II) ion. Most importantly, compounds **1**-**3** represent the first example that the Strandberg-type POMs were used as acid-catalysts in organic reaction.

Introduction

Progress in polyoxometalate (POM) chemistry has always been closely related to the functionalized POM materials. The Strandberg-type POMs, as an important subclass, have attracted significant attention due to their own structural characters, as well as their higher charges. They have been used to construct inorganic-organic hybrid materials. In recent years, many new POMs containing $\{P_2Mo_5\}$ skeleton, organic group and metal ions have been successfully synthesized.[1,2] Moreover, some important properties of these compounds are being gradually recognized. For example, Su's group investigated the electronic properties, redox properties, and relative basicity of the external oxygen atoms of the Strandberg POMs. They pointed out that the changes in the electronic properties can modify the redox properties of POMs.[3,4] In 2012, Banerjee's group first reported the proton conductivity of the Strandberg POM-based MOFs at solid state.[5] These research results will help us design, synthesize and utilize this type of POM-based materials. It is well known that POMs can be used as photocatalysts,[6] electrocatalysts,[7] and they are the most widely used as catalysts in organic synthesis, such as esterification reaction,[8] oxidation reaction[9] and protection of carbonyl compounds.[10] Protection of carbonyls as acetals or ketals is one of the most important organic reactions, and there are many methods were reported in the literatures.[11,12] In 2011, Rahimizadeh's group reported that the Preyssler-type POM is a mild and efficient catalyst for the protection of carbonyl compounds.[10] To the best of our knowledge, there is no report on the catalytic activity of the Strandberg POM used as catalyst in organic synthesis. In addition, 2,2'-biimidazole, as a polydentate ligand, is able to coordinate to transition metals with three reversible types: neutral (H_2biim), monoanion ($Hbiim^-$), and dianion ($biim^{2-}$) types,[13] but few compounds involving transition metal, H_2biim ligands, and polyoxoanions have been reported. In our previous work, we have synthesized some transition metal (TM)-H_2biim complexes-supported Strandberg-type molybdophosphates, octamolybdates, and Preyssler-type tungstophosphates.[1d,14,15] The catalytic activities of the above Preyssler-type POMs for the oxidation of cyclohexanol are preliminarily explored. As can be seen from the above examples, though the nitrogen donor ligand H_2biim has weak reduction ability, but it can be introduced into the POM skeletons for assembling hybrid materials with versatile coordination type. H_2biim is a valuable building block for constructing inorganic-organic hybrid materials by hydrogen bonding and π–π stacking interactions. So, as an extension of work, we endeavored to construct new inorganic-organic hybrid compounds based on transition metals and the $\{P_2Mo_5\}$ clusters, and further to explore their potential catalytic activities in organic synthesis. Herein, we have synthesized three Zn(II)-H_2biim/H_2O-supporting Strandberg-type POMs, and for the first time, reported $\{P_2Mo_5\}$-based catalysts used in organic synthesis, *i.e.* these POMs were used as catalysts for the protection of carbonyl compound with glycol.

Results and Discussion

Synthesis

Strandberg-type POMs, as typical oxygen-containing mono- or polydentate ligands, can coordinate with transition metals through the tetrahedral or octahedral oxygen atoms. The further introduction of organic groups will construct new hybrid structures. The

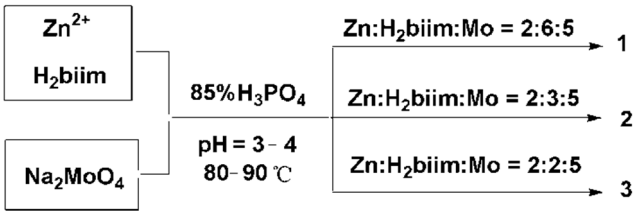

Scheme 1 Schematic representation of pathways and experimental conditions for the formations of **1-3**

nitrogen donor ligand H_2biim has versatile coordination behavior,[16] however, the synthesis of the inorganic-organic hybrid materials based on Strandberg-type polyanion and TM/H_2biim has been a great challenge. One of the main reasons is that the Strandberg-type polyanion has higher charge, and it easily precipitates when it encounters cations. Furthermore, the H_2biim ligand is easily protonated in acidic solution resulting in the decrease of its coordinating ability. During the syntheses of compounds 1-3, $Na_2MoO_4{\cdot}2H_2O$, H_2biim and $ZnSO_4{\cdot}7H_2O$ were used as starting materials, and excess H_3PO_4 was added. The effect of phosphoric acid is not only to ensure the required amounts of P for the reaction process, but also to control the pH. The synthetic strategy for compounds **1-3** is presented in Scheme 1. In the synthetic process, we found that the control of the reaction conditions played a crucial role in constructing different structures. Experiment results indicate that reasonable yields of crystalline products can be obtained at pH = 3-4. The pH of the reaction system is the key factor for the formation of the Strandberg-type structures. Lower pH values resulted in forming Keggin structures, while higher pH gave only powders containing $\{P_4Mo_6\}$ POM, which can be tested by the UV spectra (Fig. S1, ESI†). The phenomenon is similar to the literature's results,[17,18] and also indicates that $\{P_2Mo_5\}$ and $\{P_4Mo_6\}$ can be mutually transformed. Meanwhile, the concentration of the reactants is an important factor affecting the structures of the products and the coordinate modes of H_2biim ligands.

Structural analysis

As a common feature, each crystal molecule contains two $\{P_2Mo_5\}$ units. The $\{P_2Mo_5\}$ unit may be described as a nearly planar $\{Mo_5\}$ ring of five edge- and corner-sharing MoO_6 octahedra capped on either face by two PO_4 tetrahedra in a corner-sharing mode. In the single crystal structures, each Zn(II)-H_2biim/H_2O fragment supports on one side of the Strandberg-type anion linked through one terminal oxygen atom of a PO_4 tetrahedron, *i.e.* the $\{P_2Mo_5\}$ unit acts as a monodentate ligand. Though all Zn(II) ions adopt five-coordinated square-pyramidal coordination geometries, but their coordination environments are different and distorted. The asymmetric unit of **1** contains one mono-supporting $\{P_2Mo_5\}$ unit, and one and a half free H_2biim molecules, and one and a half lattice water (Fig. S2 (a), ESI†). As shown in Fig. 1, the Zn1 center coordinates with one oxygen atom (O8) from a capped PO_4 tetrahedron group (Zn1–O8 1.932(3) Å), three nitrogen atoms (N1, N2, N5) from two H_2biim ligands (Zn1–N: 2.029(5)-2.206(5) Å), and one terminal water ligand O1W (Zn1–O1W 2.251(3) Å). The two H_2biim molecules, as bidentate and monodentate ligands, provide two and one pairs of electrons, respectively. In one of the H_2biim molecules, two imidazole rings are not co-planar and distort along the C–C bond.

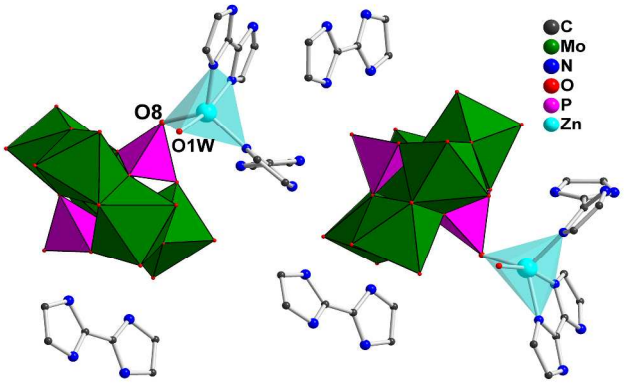

Fig. 1 Combined polyhedral and ball-and-stick representation for compound **1** (Hydrogen atoms and free water molecules have been omitted for clarity)

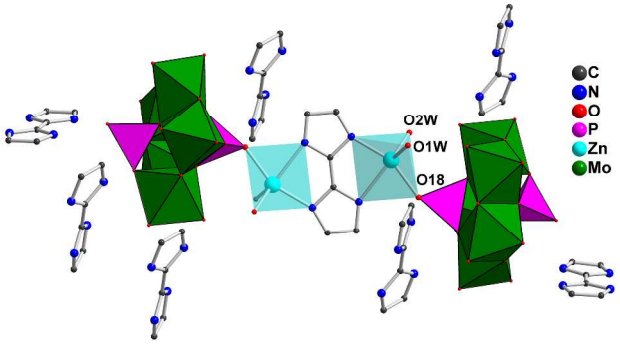

Fig. 2 Combined polyhedral and ball-and-stick representation for compound **2** (Hydrogen atoms and free water molecules have been omitted for clarity)

The N6–C7–C8–N8 torsion angle is 43.2(9)º, and the dihedral angle between the planes C12_C11_N7_C8_N8 and C10_C9_N5_C7_N6 is 46.8 º. Bond valence sum (BVS)[19,20] calculations show that the oxidation states for P, Zn and Mo atoms are +5, +2 and +6, respectively. The BVS value of the tetrahedral oxygen atom O13/O13′ is 1.24, indicating that the oxygen atom is mono-protonated. As viewed from the packing diagram in Fig. S3 (ESI†), a 3-D supramolecular framework is formed *via* strong hydrogen bonding (*e.g.* N–H···O/OW 2.566(7)-3.276(7) Å) between H_2biim ligands and the polyoxoanions or crystal water molecules, and π-π interactions between the imidazole rings of biimidazole ligands.

The unit cell of **2** contains a binuclear zinc complex based on two $\{P_2Mo_5\}$ units and one dehydrogenated 2,2'-biimidazole ligand. Fig. S2(b) (ESI†) shows the asymmetric unit of **2**. As viewed from Fig. 2, two mono-supporting Zn-$\{P_2MO_5\}$ subunits are bridged by a bi-negative tetradentate ligand μ-$[biim]^{2-}$ forming a symmetrical structure. As far as we know, such coordinate mode of 2,2'-biimidazole has not been reported in POM systems. The asymmetric Zn1 center is five-coordinated by two nitrogen atoms (N15, N16A) from a μ-$[biim]^{2-}$ ligand (Zn1–N: 2.221(7), 2.008(5) Å), and one oxygen atom (O18) from a capped PO_4 tetrahedron group (Zn1–O18 2.126(2) Å), and two terminal water ligands (Zn1–O1W, 2.055(6) Å; Zn1–O2W, 1.998(4) Å), exhibiting a strongly distorted square pyramidal geometry. Furthermore, the Zn1 shows half-occupancy. BVS calculations show that the oxidation states for P, Zn and Mo

atoms are +5, +2 and +6, respectively. The VBS value of the tetrahedral atom

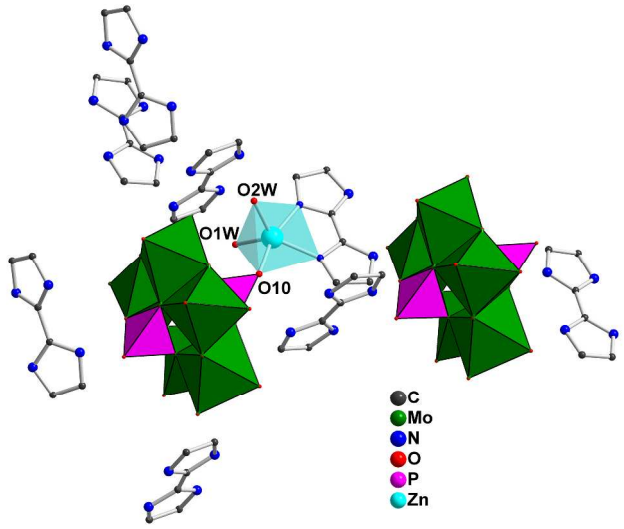

Fig. 3 Combined polyhedral and ball-and-stick representation for compound **3** (Hydrogen atoms and free water molecules have been omitted for clarity)

O13/O13′ is 1.33, indicating that the oxygen atom is mono-protonated. There also exists a 3-D supramolecular framework through π-π stacking and strong hydrogen bonding interactions (*e.g.* N–H···O/OW 2.574(3)-3.002(3) Å) (Fig. S4, ESI†).

In the crystal structure of **3,** each molecule also contains two $\{P_2Mo_5\}$ units, but **3** is not symmetrical structure when compared with **1** and **2**. The structural unit of **3** is composed of one mono-supporting $[Zn(H_2biim)(H_2O)_2(HP_2Mo_5O_{23})]^{3-}$, one isolated $[H_2P_2Mo_5O_{23}]^{4-}$, seven free H_2biim and eight lattice water molecules (see Fig. S2(c), ESI† and Fig. 3). The Zn1 atom is coordinated by two nitrogen atoms from one H_2biim ligand, one oxygen atom from a capped PO_4 tetrahedron group, and two oxygen atoms from two water molecules. The distances around Zn1 are 2.177(6) and 2.063(6) Å for Zn1–N1 and Zn1–N2, 2.094(4) Å for Zn1–O10, 2.004(5) and 2.014(5) Å for Zn1–O1W and Zn1–O2W. The Zn1 atom adopts tiny distorted square-pyramidal coordination geometry. BVS calculations gave values for P, Zn, Mo atoms are +5, +2 and +6, respectively, and the values of the tetrahedral oxygen atoms O27, O39 and O44 are 1.32, 1.35 and 1.32, respectively, indicating that the oxygen atom is mono-protonated. Fig. S5 (ESI†) exhibits a spatial arrangement of the polyoxoanions. In their packing arrangement, the $[Zn(H_2biim)(H_2O)_2(HP_2Mo_5O_{23})]^{3-}$ and $[H_2P_2Mo_5O_{23}]^{4-}$ units (namely A and B) are alternately arranged to form 2D layers with ABAB pattern. The polyoxoanions in adjacent layers situated in face to face or back to back, constructing a 3D architecture *via* extensive strong hydrogen bonding interactions (*e.g.* N–H···O/OW 2.560(6)-3.248(7) Å) among the polyanions, crystal water molecules and H_2biim units, and π-π stacking of H_2biim molecules (see Fig. S6, ESI†).

It can be seen from the above structures, the intramolecular and intermolecular hydrogen bonds play a key role in building up and stabilizing these solid frameworks, that is to say, 2,2'-biimidazole, as an interesting building block, has an important function of controlling crystal structures, and the polyoxoanion clusters make the structures becoming more innovative and more stable. Therefore, we can also say hydrogen bonded 2,2'-biimidazolate transition metal complexes can be used as a tool of crystal engineering.[13]

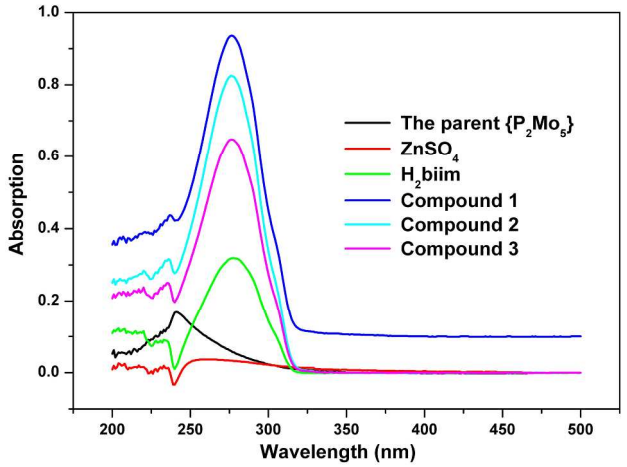

Fig. 4 Comparison of UV-visible spectra for the parent $\{P_2Mo_5\}$, $ZnSO_4$, H_2biim and **1-3** (5×10^{-5} mol L^{-1}) at pH = NaAc-HAc (pH = 4) buffer solution

Characterization

FT-IR spectroscopy. As shown in Fig. S7 (ESI†), the IR spectra of **1**–**3** are similar. The bands at 2781-3437 cm^{-1} are associated with C–H, N–H and O–H bending and stretching vibrations. Absorption peaks in the range of 1216-1647 cm^{-1} can be assigned to imidazole ring stretching of H_2biim.[13-15,17] Furthermore, all the compounds exhibit characteristic peaks of the $\{P_2Mo_5\}$ polyoxoanion: the bands at 1027-1106 cm^{-1} are attributed to ν(P–O), and strong bands at 680-694, 759-773 and 912-918 cm^{-1} are attributed to the $\nu(Mo–O_{bridging})$ and $\nu(Mo–O_{terminal})$ modes of the polyoxoanion.[1e] Small shifts in the wavelengths of the $\{P_2Mo_5\}$ characteristic peaks may due to the different coordination environments of the three compounds.

UV-Visible spectroscopy. The UV-vis absorption behaviours of the parent $\{P_2Mo_5\}$, $ZnSO_4$, H_2biim and **1-3** were analyzed using NaAc-HAc (pH = 4) buffer solution. The obtained spectra between 200 and 500 nm are presented in Fig. 4. In the visible region, no absorption bands were observed. In the UV region, the UV spectrum of the parent $\{P_2Mo_5\}$ has a strong band at *ca*. 241 nm in the range of 200-355 nm, which is attributed to the characteristic absorption of $\{P_2Mo_5\}$: the ligand-to-metal pπ-dπ charge transfer transitions (O→Mo).[18] The electronic spectrum of $ZnSO_4$ shows no absorption band. A strong band at 278 nm corresponds to π-π charge transfer transitions of H_2biim. The UV spectra of **1-3** also reveal one strong absorption band centred at *ca*. 276 nm in the range of 230-320 nm, which is assigned to the absorption behaviours of the inorganic-organic hybrid compounds based on POM and H_2biim, and the characteristic absorption of $\{P_2Mo_5\}$ are overlapped by the broad band of H_2biim.

Thermal analysis. In order to examine the thermal stabilities of **1-3**, thermal gravimetric (TG) analyses were carried out. As seen in Fig. S8 (ESI†), the TG curves of **1-3** exhibit some obvious similarities from 75 to 1,000 °C. In the temperature range of 75-568 °C, each compound shows a continuous weight loss step. The observed total weight losses for **1-3** are 39.14%,

44.36% and 42.93%, respectively. It is obvious that the weight loss is higher than the theoretical value for the removal of all

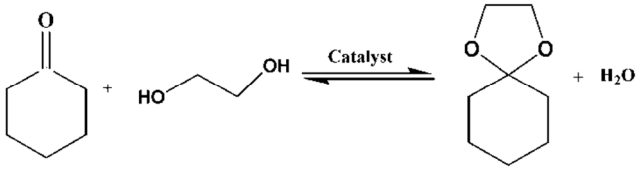

Scheme 2 Ketalization of cyclohexanone with glycol

water and H_2biim molecules (calc. 36.52%, 39.75% and 40.13%, respectively), which may be due to partial loss of phosphorus oxide resulting from the partial decomposition of the polyoxoanion.[1d] The exothermal peaks observed respectively at 494, 531 and 534 °C in the DTA curves of **1**-**3** are further proofs of the collapse of the polyoxoanion skeletons. From 300 to 360 °C, weak and strong exothermal peaks are observed at 318 and 457 °C for **1**, 330 and 449 °C for **2** and **3**, respectively, which are assigned to combustions of the H_2biim organic fragments. Additionally, three compounds continuously lost weight at temperatures higher than ~ 690 °C, which corresponds to loss of phosphorus oxide and molybdenum trioxide. In short, thermogravimetric analyses show that the title compounds have similar and high thermal stabilities; the decomposition temperatures of the polyoxoanions are about 700 °C, showing that the transition metal complexes help to stabilize the inorganic-organic framework.

Catalytic activities of three compounds

The acid-catalytic protection of carbonyl group is a key reaction in multi-step synthesis of many important organic compounds (Scheme 2).[21,22] It is well known that some protonic acids: anhydrous HCl, H_2SO_4, *etc*. were generally used as catalysts for protection of carbonyl groups. These acids cannot be reused or recycled, and produce large amounts of waste and pollution, especially may cause serious corrosion of equipment. Therefore, the development of more efficient, recyclable, and environmental pollution-free catalyst is a long-term goal.

POMs, as a kind of multifunctional catalysts, have been applied to many organic reactions, mainly due to their strong redox and acidic properties. How about **1**-**3** based on the $\{P_2Mo_5\}$ units? Firstly, we used them including the parent $\{P_2Mo_5\}$ as heterogeneous catalysts in the oxidation of cyclohexanol to cyclohexanone to evaluate their oxidative catalysis activities. It was found that the cyclohexanone yield was much lower (< 15 %) compared with those of our reported POMs.[15,23] Then, we test them in the synthesis of cyclohexanone ethylene ketal. Delightedly, they exhibit better catalytic activities in this acid-catalyzed reaction. For compound **2**, 99% of yield was obtained (Table 1, entry 4). For compound **1** and **3**, 86% and 95% of yields were obtained, respectively (Table 1, entry 3/5). The parent $\{P_2Mo_5\}$ and $ZnSO_4$ were also checked as a control experiment, they showed a low catalytic activities (Table 1, entry 1/2). The reaction conditions, such as reaction time, the molar ratio of starting material, and the amount of catalyst or water-carring agent were systemically explored (Figs. S9-S12, ESI†). For the three compounds, similar catalytic performances presented. As shown in Fig. S9 and Fig. S10 (ESI†), the yields of ketals increased quickly with the increasing of time within 2 hours, and the cyclohexanone-glycol molar ratio of 1:1.4 is a suitable substrate molar one. The amount of catalyst was one of important

Table 1 Catalytic performance of the catalysts (**1-3)** for the synthesis of cyclohexanone ethylene ketal

Entry	Catalyst	Solubility	Time (h)	yield (%)
1	$\{P_2Mo_5\}$	insoluble	2	50
2	$ZnSO_4$	insoluble	2	10
3	Compound **1**	insoluble	2	86
4	Compound **2**	insoluble	2	99
5	Compound **3**	insoluble	2	95

Reaction conditions: the molar ratio of the catalyst (based on Mo/Zn) to cyclohexanone was 1:300, and cyclohexanone to glycol was 1:1.4 (0.05 mol of cyclohexanone); water-carring agent: 10 mL of cyclohexane; reaction temperature: 95-100 °C.

Table 2 Synthesis of cyclohexanone ethylene ketal by catalysts **1**-**3** for different cycles

Catalyst	Yield (%)			
	Fresh	Cycle 1	Cycle 2	Cycle 3
Compound **1**	86.0	84.2	82.5	80.4
Compound **2**	98.8	95.6	90.2	84.8
Compound **3**	95.4	92.1	88.7	82.4

Reaction conditions: the molar ratio of the catalyst (based on Mo) to cyclohexanone was 1:300; *n*(cyclohexanone): *n*(glycol) = 1:1.4 (0.05 mol of cyclohexanone); water-carring agent: 10 mL of cyclohexane; reaction time: 2 h; reaction temperature: 95-100 °C.

affective factors, when the catalyst was 1/300 of cyclohexanone, for compounds **1**-**3**, the maximum yields of cyclohexanone ethylene ketal were 86 %, 99% and 95%, respectively (Fig. S11, ESI†). Taking compound **2** as an example, we have investigated the amount of the water-carring agent, it can be seen that 10 mL of cyclohexane water-carring agent is the best dosage (Fig. S12, ESI†). The optimum conditions for the synthesis of cyclohexanone ethylene ketal with as catalyst were as follows: 1) the cyclohexanone-glycol molar ratio is 1:1.4; 2) the molar ratio of the catalyst to cyclohexanone is 1:300; 3) a reaction temperature of 95-100 °C, and a reaction time of 2 h, and 10 mL of cyclohexane water-carring agent. Moreover, we found that these POM catalysts maintain the catalytic activities during the later cycles, and did not significantly change after cycles (Table 2), which indicates that the $\{P_2Mo_5\}$ skeleton has higher stability, and can be further proved by IR and PXRD. For example, the IR spectra and PXRD of the fresh and the used catalyst**s** are shown in Fig. S13 (ESI†) and Fig. S14 (ESI†): the IR characteristic peaks of the $\{P_2Mo_5\}$ also maintained, and the diffraction peaks on the pattern correspond well in peak positions of PXRD, which illustrated that the skeletons of these catalysts still keep before and after reaction compared with the parent $\{P_2Mo_5\}$ polyanion.

Experimental

Materials and methods

All chemicals were of reagent grade as received from commercial sources and used without further purification. C, H and N elemental analyses were performed on a Perkin-Elmer 2400 CHN elemental analyzer and P, Zn and Mo were analyzed on a Plasma-Spec-II ICP atomic emission spectrometer. The infrared spectra

were recorded on KBr pellets with a Bruker AXS TENSOR-27 FTIR spectrometer in the range of 4000-400 cm^{-1}. UV spectra were performed on a Lambda 35 UV-Visible spectrophotometer. Single crystal X-ray diffraction data were collected on a Bruker Smart APEX II X-diffractometer equipped with graphite-monochromated Mo Kα radiation (λ = 0.71073 Å). X-ray powder diffraction data was collected on a Bruker AXS D8 Advance diffractometer using Cu Kα radiation (λ = 1.5418 Å) in the 2θ range of 5–60 º with a step size of 0.02º. TG analyses were performed on a Pyris Diamond TG-DTA thermal analyzer in air with a heating rate of 10 °C min^{-1}. The yield of cyclohexanone ethylene ketal was confirmed on a JK-GC112A Gas Chromatograph.

Syntheses of compounds

Compound 1. $ZnSO_4·7H_2O$ (0.575 g, 2.0 mmol) and H_2biim (0.805 g, 6.0 mmol) were dissolved in 70 mL of water, and the mixture was stirred for 30 min. Then $Na_2MoO_4·2H_2O$ (1.210 g, 5.0 mmol) was added with vigorous stirring. To this solution the concentrated H_3PO_4 was added dropwise until pH = 3-4 under continuous stirring. The resulting solution was stirred at 80-90 °C for an additional 2 h and was filtered, and the colourless filtrate was kept under ambient conditions for ten days. Colorless block crystals were obtained. Yield: 76% based on Mo. Elemental analysis, Found: C, 16.8; H, 2.1; N, 13.1; Zn, 4.3; P, 4.2; Mo, 32.2. Calc. for $C_{42}H_{60}Mo_{10}N_{28}O_{51}P_4Zn_2$: C, 16.9; H, 2.0; N, 13.1; Zn, 4.4; P, 4.15; Mo, 32.1%. FT IR (KBr pellet), cm^{-1}: 3437(m), 3149(s), 2971(m), 2923(m), 2781(m), 1647(w), 1548(w), 1428(w), 1316(w), 1097(m), 1055(m), 916(s), 773(m), 694(s), 580(w), 540(w).

Compound 2/3. The syntheses of compound **2** and **3** were the same as above, except that the reactions were carried out in a molar ratio of 2:3:5 and 2:2:5, i.e. H_2biim were reduced to 0.403 g (3.0 mmol) and 0.268 g, (2.0 mmol), respectively. After slowly cooling to room temperature, the resulting solutions were filtered and the filtrates were maintained at room temperature. The colorless plate crystals for **2** and faint yellow plate crystals for **3** were isolated after 2-3 days. Yields of **2** and **3** are 65% and 72% (based on Mo), respectively.

Elemental analyses for **2**, Found: C, 17.9; H, 2.5; N, 13.8; Zn, 2.2; P, 3.7; Mo, 31.4. Calc. for $C_{45}H_{73}Mo_{10}N_{30}O_{55}P_4Zn$: C, 18.4; H, 2.4; N, 14.3; Zn, 2.1; P, 4.0; Mo, 30.7%. FT IR (KBr pellet), cm^{-1}: 3413(m), 3139(s), 3017(m), 2932(m), 1642(m), 1581(w), 1538(w), 1496(w), 1417(w), 1320(w), 1216(w), 1100(m), 1033(s), 918(s), 759(m), 680(s).

Elemental analyses for **3**, Found: C, 18.3; H, 2.6; N, 14.1; Zn, 2.1; P, 3.9; Mo, 30.4. Calc. for $C_{48}H_{80}Mo_{10}N_{32}O_{57}P_4Zn$: C, 18.3; H, 2.5; N, 14.2; Zn, 2.1; P, 3.9; Mo, 30.5%. FT IR (KBr pellet), cm^{-1}: 3413(m), 3139(s), 3024(m), 2944(m), 2798(m), 1642(m), 1587(w), 1538(w), 1450(w), 1423(w), 1320(w), 1216(w), 1106(m), 1027(s), 912(s), 759(s), 680(s).

Single-crystal X-ray diffraction

The structures were solved by direct methods and refined by the full-matrix least-squares fitting on F^2 using SHELXTL-97.[24,25] An empirical absorption correction was applied using the SADABS program. Cell parameters were obtained by the global refinement of the positions of all collected reflections. Hydrogen atoms on C or N atoms were added in calculated positions. Crystal data and structure refinement parameters of compounds **1-3** are listed in Table 3. Selected bond lengths and angles are given in Tables S1-S3 (ESI†). Hydrogen bonds are listed in Tables S4-6 (ESI†). During the refinement of compounds **1-3**, protonated N atoms on the H_2biims were determined by the charge-balance considerations. All hydrogen atoms on water molecules were directly included in the final molecular formula. CCDC reference numbers: 962343, 962344 and 962345.

Table 3 Crystal and Refinement Data for Compounds **1-3**

	1	**2**	**3**
Formula	$C_{42}H_{60}Mo_{10}N_{28}O_{51}P_4Zn_2$	$C_{48}H_{74}Mo_{10}N_{32}O_{55}P_4Zn$	$C_{48}H_{78}Mo_{10}N_{32}O_{56}P_4Zn$
Formula weight	2987.24	3128.04	3148.09
T/K	298(2)	296(2)	298(2)
Wavelength/Å	0.7107	0.7107	0.7107
Crystal system	Orthorhombic	Triclinic	Triclinic
Space group	*Pnn*2	*P*$\bar{1}$	*P*$\bar{1}$
a /Å	20.086(2)	11.1120(16)	11.1295(8)
b/Å	21.185(2)	11.3558(16)	20.2353(15)
c/Å	10.5333(12)	21.988(3)	21.9751(16)
α/°	90.00	100.062(2)	76.875(1)
β /°	90.00	93.345(2)	86.542(1)
γ /°	90.00	116.935(2)	87.499(1)
V /Å^3, Z	4482.1(8), 2	2405.5(6), 1	4808.6(6), 2
D_c /g cm^{-3}, F_{000}	2.213, 2911	2.159, 1536	2.174, 3095
GOF	1.036	1.098	1.051
Reflections collected	25544	12541	26194
Unique data, R_{int}	9641, 0.0424	8809, 0.0174	18473, 0.0199
θ Range(°)	2.16 to 27.00	2.15 to 25.50	1.91 to 26.00
$R_1(I > 2\sigma(I))$ [a]	0.0344	0.0335	0.0430
wR_2 (all data)[a]	0.0774	0.0892	0.1293

[a] $R_1 = \sum||F_0|-|F_C||/\sum|F_0|$; $wR_2 = \sum[w(F_0^2-F_C^2)^2]/\sum[w(F_0^2)^2]^{1/2}$

Catalytic experiment

Protection for the carbonyl group. Acid-catalyzed synthesis of cyclohexanone ethylene ketal was used as a model reaction of to evaluate the catalytic performances of **1-3**. A typical procedure of the catalytic activity test is as follows: the catalyst (compound **1,** 0.050 g, 0.017 mmol) was added to a mixture of cyclohexanone (4.91 g, 0.05 mol), glycol (4.34 g, 0.07 mol) and cyclohexane (10 mL) in a 50 mL three-necked round-bottom flask fitted with a Dean-Stark apparatus to remove the water continuously from the reaction mixture. After completion of the reaction, the heterogeneous catalyst remained at the bottom of the reaction vessel and was easily separated from the organic phase containing product by decantation. The recovered catalyst was dried at 200 °C for 2 h and reused in a new reaction under identical experimental conditions. Each of the procedures was repeated for three cycles. The products obtained were characterized by gas chromatography.

Repeating the above experiment under the same conditions except that compound **1** was replaced by compound **2**/**3**, the parent polyoxometalate $\{P_2Mo_5\}$, and raw materials, *i.e.* $ZnSO_4$ (note: maintaining the molar ratio of Mo or Zn: cyclohexanone is 1:300, and these catalysts were pretreated by being dried at 200 °C for 2 h), respectively.

Conclusions

In summary, compounds **1-3** display the transition metal-organic complex mono-supporting Strandberg-type structural features. The successful syntheses of three compounds show that the zinc-H_2biim/H_2O complex can be assembled with polyoxoanion, forming new interesting structures. Our experimental results show that these Strandberg-type POMs, as catalysts, showed better catalytic performances in acid-catalyzed organic reaction. The recycled catalyst was used without observation of appreciable loss in its catalytic activities. In addition, **1-3** show higher catalytic activity compared with the catalytic activities of the raw material $ZnSO_4$ and their parent $\{P_2Mo_5\}$, which proved that the synergistic effect of $\{P_2Mo_5\}$ and transition metal complex in the inorganic-organic hybrid compounds leads to the enhanced catalytic properties. Further work on the introduction of other metals as well as organonitrogen ligands is now going on in our group.

Acknowledgements

This work was financially supported by the Natural Science Foundation of Liaoning Province (No. 2013020128), and the Foundation of Education Department of Liaoning Province (No. L2013414). We are also thankful to Professor Yan Xu (Nanjing Technology University) and Professor Yang-Guang Li (Northeast Normal University) for assistance with solving the crystal structures.

Notes and references

* *School of Chemistry and Chemical Engineering, Liaoning Normal University, Dalian116029, China. Fax: +86 411 82156550; Tel: +86 411 82158559; E-mail: zhanglancui@lnnu.edu.cn; chemzhu@sina.com*

† Electronic Supplementary Information (ESI) available: ORTEP views and packing views of **1-3**; Infrared spetra and TG-DTA of **1-3**. The optimal catalytic curves. For ESI and crystallographic data in CIF or other electronic format see DOI: 10.1039/b000000x/

1 *(a)* H. J. Jin, B. B. Zhou, Y. Yu, Z. F. Zhao and Z. H. Su, *Cryst. Eng. Comm*., 2011, **13**, 585; *(b)* Y. Lu, J. Lü, E. B. Wang, Y. Q. Guo, X. X. Xu and L. Xu, *J. Mole. Struct.*, 2005, **740**, 159; *(c)* C. Qin, X. L. Wang, L. Yuan and E. B. Wang, *Cryst. Growth. Des*., 2008, **8**, 2093; *(d)* Y. Wang, L. C. Zhang, Z. M. Zhu, N. Li, A. F. Deng and S. Y. Zheng, *Trans. Met. Chem.*, 2011, **36**, 261; *(e)* J. Thomas and A. Ramanan**,** *Cryst. Growth. Des.*, 2008, **8**, 3390.

2 *(a)* P. DeBurgomaster, A. Aldous, H. X. Liu, C. J. O'Connor and J. Zubieta, *Cryst. Growth. Des*., 2010, **10**, 2209; *(b)* N. G. Armatas, W. Ouellette, K. Whitenack, J. Pelcher, H. X. Liu, E. Romaine, C. J. O'Connor and J. Zubieta, *Inorg. Chem*., 2009, **48**, 8897.

3 S. M. Yue, L. K. Yan, Z. M. Su, G. H. Li, Y. G. Chen, J. F. Ma, H. B. Xu and H. J. Zhang, *J. Coord. Chem.*, 2004, **57**, 123.

4 L. K. Yan, Z. M. Su, K. Tan, M. Zhang, L. Y. Qu and R. S. Wang, *Int. J. Quant. Chem*., 2005, **105**, 37.

5 C. Dey, T. Kundu and R. Banerjee, *Chem. Commun*., 2012, **48**, 266.

6 S. J. Li, S. M. Liu, S. X. Liu, Y. W. Liu, Q.Tang, Z. Shi, Shuxin Ouyang and J. H. Ye, *J. Am. Chem. Soc*., 2012, **134**, 19716.

7 *(a)* S. Yao, Z. M. Zhang, Y. G. Li and E. B. Wang, *Dalton Trans.*, 2010, **39**, 3884-3889; *(b)* L. C. Zhang, S. L. Zheng, H. Xue, Z. M. Zhu, W. S. You, Y. G. Li and E. B. Wang, *Dalton Trans*., 2010, **39**, 3369; *(c)* 20 X. L. Wang, J. Li, A. X. Tian, H. Y. Lin, G. C. Liu and H. L. Hu, *Inorg. Chem. Commun*., 2011, **14**, 103.

8 *(a)* F. F. Bamoharram, M. M. Heravi, M. Roshani, M. Jahangir and A. Gharib, *Appl. Catal. A: General*, 2006, **302**, 42; *(b)* F. F. Bamoharram, M. M. Heravi, M. Roshani, A. Gharib and M. Jahangir, *J. Mol. Catal. A: Chem.*, 2006, **252**, 90. *(c)* S. S. Wu, P. Liu, Y. Leng and J. Wang, *Catal. Lett*., 2009, **132**, 500; *(d)* C. Y. Sun, S. X. Liu, D. D. Liang, K. Z. Shao, Y. H. Ren and Z. M. Su, *J. Am. Chem. Soc*., 2009, **131**, 1883.

9 *(a)* Y. Leng, J. Wang, D. R. Zhu, M. J. Zhang, P. P Zhao, Z. Y. Long and J. Huang, *Green Chem*., 2011, **13**, 1636; *(b)* Y. Ding, W. Zhao, W. F. Song, Z. X. Zhang and B. C. Ma, *Green Chem*., 2011, 13, 1486.

10 M. Rahimizadeh, T. Bazazan, A. Shiri, M. Bakavoli and H. Hassani, *Chin. Chem. Lett*., 2011, **22**, 435.

11 G. Sartori, R. Ballini, F. Bigi, G. Bosica, R. Maggi and P. Righi, *Chem. Rev.*, 2004, **104**, 199.

12 M. Zahouily, A. Mezdar, J. Rakik, A. Elmakssoudi, A.Rayadh and S. Sebti, *J. Mol. Cata. A*: *Chem.*, 2005, **233**,43.

13 M. Tadokoro and K. Nakasuji, *Coord. Chem. Rew*., 2000, **198**, 2058.

14 J. L. Wang, L. C. Zhang, X. H. Li, C. C. You and Z. M. Zhu, *Transition Met. Chem.*, 2012, **37**, 303.

15 C. Y. Yang, L. C. Zhang, Z. J. Wang, L. Wang, X. H. Li and Z. M. Zhu, *J. Solid State Chem*., 2012, **194**, 270.

16 *(a)* J. R. Galán-Mascarós and K. R. Dunbar, *Angew. Chem., Int. Ed*., 2003, **42**, 2289; *(b)* B. H. Ye, B. B. Ding; Y. Q. Weng and X. M. Chen, *Cryst. Growth Des*., 2005, **5**, 801-806.

17 K. Yu, B. B. Zhou, Y. Yu, Z. H. Su, H. Y. Wang, C. M. Wang, and C. X. Wang, *Dalton Trans.*, 2012, **41**, 10014.

18 J. Y. Niu, J. C. Ma, J. W. Zhao, P. T. Ma and J. P. Wang, *Inorg. Chem. Commun*., 2011, **14**, 474.

19 I. D. Brown, and D. Altermatt, *Acta*. *Cryst*., 1985, *B***41**, 244.

20 H. H.Thorp, *Inorg. Chem*., 1992, 31, 1585.

21 D. J. Tao, Z. M. Li, Z. Cheng, N. Hu, X. S. Chen. *Ind*. *Eng*. *Chem. Res*., 2012, **51**, 16263.

22 J. H. Liu, X. F. Wei, Y. L. Yu, J. L. Song, X. Wang, A. Li, X. W. Liu, W. Q. Deng, *Chem*. *Commun*., 2010, **46**, 1670.

23 H. Yang, L. C. Zhang, L. Yang, X. L. Zhang, W. S. You and Z. M. Zhu, *Inorg. Chem. Comm*., 2013, **29**, 33.

24 G. M. Sheldrick, SHELXL97, program for crystal structure refinement. University of Gottingen, Germany, 1997.

25 G. M. Sheldrick, SHELXS97, program for crystal structure solution. University of Gottingen, Germany, 1997.